

On the assessment of local tumor response to neoadjuvant chemotherapy

Ziemowit Klimonda *, Piotr Karwat *, Katarzyna Dobruch-Sobczak * †,
Hanna Piotrkowska-Wróblewska * and Jerzy Litniewski *,

* Institute of Fundamental Technological Research, Polish Academy of Sciences, Warsaw, Poland

† Maria Skłodowska-Curie Memorial Cancer Centre and Institute of Oncology, Warsaw, Poland

Abstract—If a malignant tumor is detected, the patient is often given neoadjuvant chemotherapy (NAC) before surgery. The effectiveness of NAC is estimated using tumor size changes. However, such a method is not always reliable, so other techniques are being investigated. The paper shows how to assess the response of different tumor areas to therapy based on the analysis of scattered ultrasound signals. Understanding the local response of the tumor can help to evaluate the effectiveness of therapy. The study used a set of raw ultrasound data from 48 tumors undergoing NAC. Ultrasound scanner was used to collect RF data before the start of NAC and after each drug administration. After therapy, tumors were resected and histopathologically evaluated. The percentage of residual malignant cells (RMC) in each lesion was estimated and used for assessing the NAC effectiveness. The set of tumors was divided into a training and a test sets. In the training set each tumor Region of Interest (ROI) was divided into small square pieces – patches, and labelled as responding or non-responding basing on RMC of the tumor. Then 357 statistical and texture features were estimated from each patch. The support vector machines binary classifier (SVM) was trained on data collected after the 3rd drug administration. The efficiency of the classifier using a different number of features in the range from 2 to 100 has been tested. The classifier was then used to determine the probability of high RMC of tumor patches from the test set. In this way, parametric images of tumors were obtained, showing the spatial distribution of the probability of a given area being unresponsive to treatment. The ‘patch approach’ allows the use of a very large set of predictors without the risk of overfitting – although the number of tumors in the set was not very large, the number of patches obtained from them was. Spatial distribution of non-responsiveness probability can be a base for detection of non-responding tumors. A simple predictor based on 70th percentile of probability of non-responsiveness after the 3rd dose resulted in a classification with an area under the ROC curve of 0.92, indicating potential for identifying non-responding tumors.

Index Terms—breast cancer, chemotherapy monitoring, quantitative ultrasound

I. Introduction

Neoadjuvant chemotherapy (NAC) of a breast cancer is a therapy given before surgical removal of the tumor. The primary goal of this approach is to reduce the size of the tumor, which facilitates the surgical operation and increases the chances of breast conservation. Typically NAC consists of several courses of drug administered at regular time intervals. Monitoring the effectiveness

of NAC is an important issue. Early detection of non-responsive tumors (i.e. those resistant to NAC), would enable quick adjustment of treatment by changing the drug or help expedite the decision to discontinue therapy and performing surgery. In case of non-responsive tumors, delaying surgery raises the risk of metastasis. Currently, evaluation is based on changes in tumor size, and it is often assessed using ultrasound (US) imaging [1]. However, this method is not always optimal. Efforts are being made to improve the assessment of NAC performance by using the physical and statistical parameters obtained from ultrasound images – methods referred to as quantitative ultrasound (QUS) – to characterize tumor tissue [2]–[4].

This study tested an approach in which tumor Region of Interest (ROI) on US image is divided into small square fragments – patches. Patches were assigned into ‘responding’ and ‘non-responding’ categories based on histopathological examination of the tumor, and then the classifier was trained. The general aim was to develop a method for imaging the local tumor response to therapy. The nature of this response, e.g. whether the response is uniform throughout the tumor or whether there are ‘resistant’ foci, seems to be an interesting direction of research towards better monitoring of tumor changes during NAC.

II. Methods

A. Data acquisition

US data were collected from 48 breast cancers undergoing NAC. All patients provided an informed consent to participate in the study. This study was approved by the Ethical Committee at the Maria Skłodowska-Curie Memorial Cancer Centre and Institute of Oncology, Warsaw, Poland.

US data were collected before each subsequent course of the chemotherapy. The number of courses for each patient was not equal and depended on physician’s decision, however in general the number of courses was more than 3. Scanning was performed by an experienced radiologist following the guidelines of the American College of Radiology (BI-RADS lexicon) [5] and the standards of the Polish Ultrasound Society [6]. Raw radio-frequency (RF) data were collected using Ultrasonix[®] SonixTOUCH scanner (Ultrasonix Medical Corporation, Canada) equipped with

This study was supported by the National Science Center of Poland (grant 2019/35/B/ST7/03792).

the L14-5/38 linear probe. Sampling frequency was equal to 40 MHz. Each tumor was scanned in four planes: radial, radial+45°, anti-radial and anti-radial+45°. All processing was carried out in the Matlab® R2021a environment. After the treatment each tumor was surgically removed and then histopathologically assessed by an experienced pathologist. The Assessment included, among others, the percentage of the remaining malignant cells (RMC). This parameter was used in the study as the indicator of tumor response to the therapy. RMC values ranged from 0 to 100, where 0 means that no viable cancer cells were found in the observed tumor tissue fragments, while 100 means that the examined fragments were completely occupied by living tumor cells. In this study tumors were arbitrarily classified as non-responding when the RMC was higher or equal to 70.

B. Data processing

Each RF image acquired after third NAC course was pre-processed to B-mode by computing the amplitude envelope using Hilbert transform and applying the decibel compression. The masks defining the region of interest (ROI) – area corresponding to a tumor location – was marked by the same radiologist who performed the US examination. The tumor dataset was divided into 5 folds and processed in k-fold manner [7] – each fold defined the division of the tumor dataset into the training and test sets. A collection of square fragments – patches – was extracted from each tumor ROI in the training and test sets. The patch size was 2x2 mm, and patches overlapped with a step equal to 0.5 mm. Each patch in the training and test set was assigned an RMC value equal to that of the tumor from which the patch was derived. The numbers of patches are given in table I. Each patch was processed by

TABLE I
Patches numbers in subsequent folds

fold#	train set		test set	
	resp#	non-resp#	resp#	non-resp#
1	23655	16039	9324	6784
2	25691	18939	7288	3884
3	28690	18956	4289	3867
4	23711	17652	9268	5171
5	30169	19706	2810	3117

a set of parameter estimators. The output of all estimators processing a single patch forms a vector (an observation) with 357 elements (features). Estimators will be described in the next subsection. The binary label was assigned to each observation basing on the patch RMC – 1 for RMC higher or equal to 70, 0 otherwise. Then the number of features was reduced by ranking features using Chi-2 test and taking the first n most important. The n in range from 2 to 100 were tested in the study. Then binary classifier was trained on the training observations. In this study the supported vector machines (SVM) classifier was used [7]. The imbalanced training set problem was addressed

by modifying cost matrix to reflect the proportions of responding and non-responding patches. The classifier was then tested on the observations derived from the test patches. The performance of the classifier was evaluated using area under the ROC curve (AUC) [8].

In the next step, the classifier was used to create parametric images of tumors from the test set. These images show spatial distributions of the probability that given patch comes from 'non-responding region' of a tumor. These 'probability images' were the base for tumor classification to 'responding' or 'non-responding' class. In this study, the 70 percentile from probability distribution was estimated and used as a score for ROC calculation. The performance of this tumor classifier was also evaluated using AUC.

C. Estimators

The set of estimators consisted of 14 statistical and textural groups of estimators. Large number of estimators was taken from BUSAT toolbox [9], however they were re-implemented to allow using the GPU functionality of Matlab® R2021a. Specifically following estimators were used: auto-correlation, auto-covariance [10], complexity curve features [11], fractal features [12], Laws energy features [13], and Gray-Level Co-occurrence Matrix (GLCM) parameters [14]. Additionally the set of estimators contained the Nakagami [15] and k-homodyned [16] distribution parameters, mean, standard deviation, entropy [17], and statistical moments from 2 to 4. The Nakagami and k-homodyned estimators were used on amplitude data with no decibel compression. The texture GLCM parameters were estimated separately vertically and horizontally, and for 6 different pixel offsets, corresponding to distance 0.075, 0.15, 0.3, 0.45, 0.6 and 0.75 mm. The summary of used estimators is given in table II.

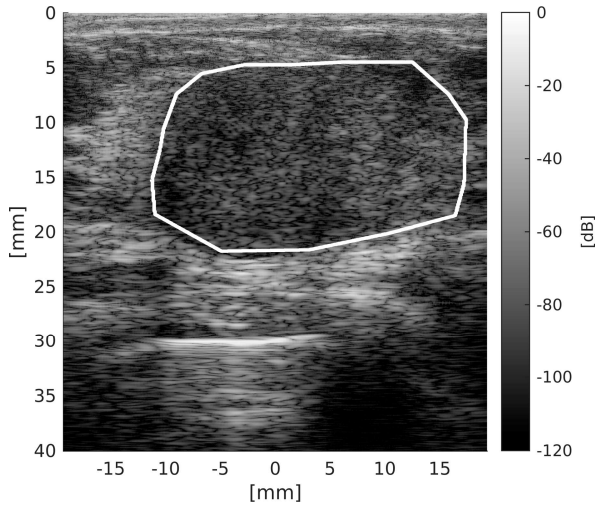
TABLE II
Estimators and number of output features

estimator	features#	estimator	features#
mean	1	k-homodyned	2
std	1	autocorrelation	1
2 nd moment	1	autocovariance	35
3 rd moment	1	complex curvature	5
4 th moment	2	Laws energy	70
entropy	1	fractal features	8
Nakagami	2	texture GLCM parameters	228

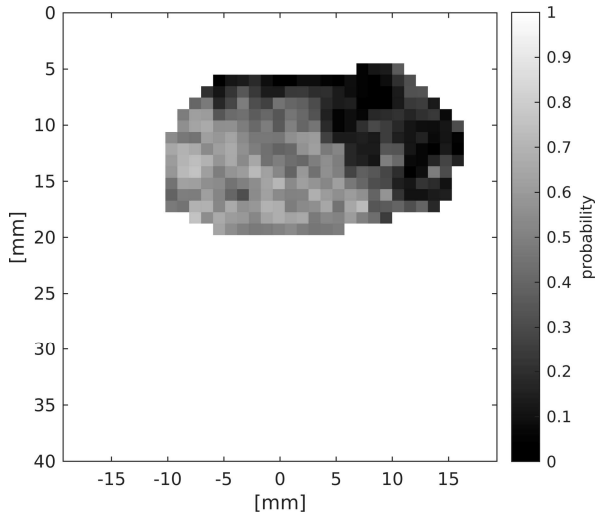
III. Results

The example of probability images for responding and non-responding tumors are presented in Fig.1 and Fig.2.

The changes of classification performance – both for patches and probability images – with increasing number of features are shown in Fig.3.



(a)



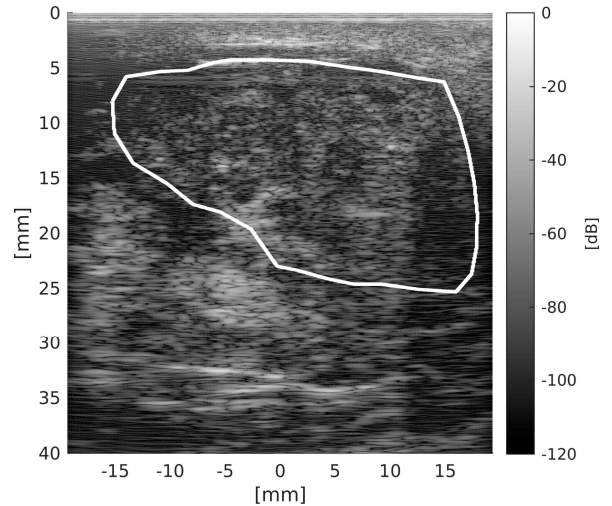
(b)

Fig. 1. (a) Bmode image with marked tumor and (b) the spatial distribution of the probability of a poor response to therapy in responding (RMC = 0%) tumor after 3rd NAC.

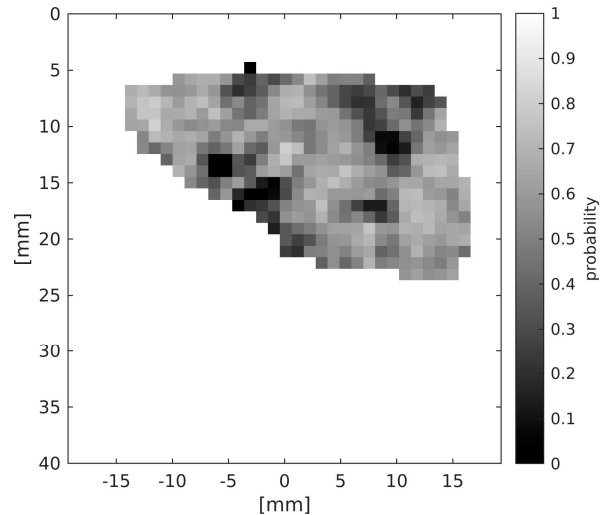
IV. Discussion

The presented tumors are characterized by different probability distributions. The image of the responding tumor (Fig.1(b)) shows a large, compact dark area on the right side of the tumor, while the image of the non-responding tumor (Fig.2(b)) shows the low-probability areas much smaller and diffuse. This suggests that the analysis of the texture of probability distributions may carry additional information, the use of which may improve the operation of the tumor classifier.

The plots presenting the efficiency of the method depending on the adopted number of features show that an unlimited increase in the number of features is not justified (Fig.3). Based on the trend of AUC vs. number of features relationship (Fig.3(b)), it seems that the tumor classifier



(a)



(b)

Fig. 2. (a) Bmode image with marked tumor and (b) the spatial distribution of the probability of a poor response to therapy in non-responding (RMC = 100%) tumor after 3rd NAC.

performance reaches its optimum around 20 to 30 features. When using 20 features the tumor classifier performance is characterized by AUC equal 0.92. Further increasing the number of features does not increase the performance. In addition, this relationship is non-monotonic, i.e. adding some features may degrade performance. This suggests that the feature selection method used was not optimal. However, one should remember about a fairly wide error channel, which makes it impossible to draw more firm conclusions.

In this work, we used a brute-force approach i.e. predictors were automatically selected from a large set of potential features. The method used to select relevant features was simple and quick, but probably non-optimal. In addition, the patch classification method (SVM) was

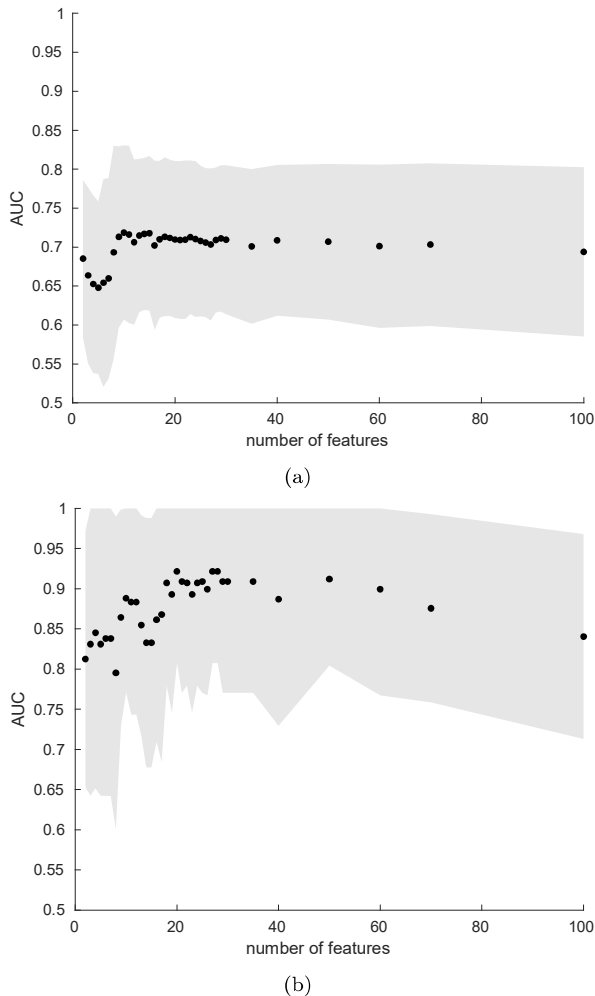


Fig. 3. AUC changes with increasing number of features used for classification of (a) patches and (b) tumors. The errorband is marked in gray.

chosen arbitrarily - it is possible that other methods work better. Finally, the tumor classifier (percentile based) was very simple, however this work is about showing the proof of concept. We expect texture analysis of probability images to provide much more information compared to a simple percentile.

V. Conclusions

The subject of the study is the method of estimating the local tumor response to neoadjuvant chemotherapy. The paper presents the results of the SVM classifier trained on a set of small US image patches of a tumor. Thanks to this approach, it was possible to use a very large set of predictors without the risk of overfitting, and to obtain probability distributions showing where a given tumor does not respond to therapy. Spatial distribution of non-responsiveness probability can be a base for detection of non-responding tumors, and can be used as a tool for monitoring the effectiveness of therapy.

Acknowledgment

This study was supported by the National Science Center of Poland (grant 2019/35/B/ST7/03792).

References

- [1] V. Romeo, G. Accardo, T. Perillo, L. Basso, N. Garbino, E. Nicolai, S. Maurea, and M. Salvatore, "Assessment and prediction of response to neoadjuvant chemotherapy in breast cancer: A comparison of imaging modalities and future perspectives," *Cancers*, vol. 13, no. 14, p. 3521, 2021.
- [2] L. Sannachi, H. Tadayyon, A. Sadeghi-Naini, W. Tran, S. Gandhi, F. Wright, M. Oelze, and G. Czarnota, "Non-invasive evaluation of breast cancer response to chemotherapy using quantitative ultrasonic backscatter parameters," *Medical image analysis*, vol. 20, no. 1, pp. 224–236, 2015.
- [3] A. Dasgupta, S. Brade, L. Sannachi, K. Quiaoit, K. Fatima, D. DiCenzo, L. O. Osapoetra, M. Saifuddin, M. Trudeau, S. Gandhi et al., "Quantitative ultrasound radiomics using texture derivatives in prediction of treatment response to neoadjuvant chemotherapy for locally advanced breast cancer," *Oncotarget*, vol. 11, no. 42, p. 3782, 2020.
- [4] H. Taleghamar, S. A. Jalalifar, G. J. Czarnota, and A. Sadeghi-Naini, "Deep learning of quantitative ultrasound multiparametric images at pre-treatment to predict breast cancer response to chemotherapy," *Scientific reports*, vol. 12, no. 1, pp. 1–13, 2022.
- [5] E. Mendelson, M. Böhm-Vélez, W. Berg, G. Whitman, M. Feldman, H. Madjar et al., "Acr bi-rads® ultrasound," *ACR BI-RADS® Atlas, Breast Imaging Reporting and Data System*. Reston, VA, American College of Radiology, vol. 149, 2013.
- [6] W. Jakubowski, K. Dobruch-Sobczak, and B. Migda, "Standards of the polish ultrasound society—update. sonomammography examination," *Journal of Ultrasonography*, vol. 12, no. 50, p. 245, 2012.
- [7] T. Hastie, R. Tibshirani, J. H. Friedman, and J. H. Friedman, *The elements of statistical learning: data mining, inference, and prediction*. Springer, 2009, vol. 2.
- [8] T. Fawcett, "An introduction to roc analysis," *Pattern Recognition Letters*, vol. 27, pp. 861–874, 2006.
- [9] A. Rodríguez-Cristerna, W. Gómez-Flores, and W. C. de Albuquerque-Pereira, "Busat: A matlab toolbox for breast ultrasound image analysis," in *Pattern Recognition: 9th Mexican Conference, MCP R 2017, Huatulco, Mexico, June 21–24, 2017, Proceedings 9*. Springer, 2017, pp. 268–277.
- [10] R.-F. Chang, W.-J. Wu, W. K. Moon, and D.-R. Chen, "Improvement in breast tumor discrimination by support vector machines and speckle-emphasis texture analysis," *Ultrasound in medicine & biology*, vol. 29, no. 5, pp. 679–686, 2003.
- [11] A. V. Alvarenga, W. C. Pereira, A. F. C. Infantosi, and C. M. Azevedo, "Complexity curve and grey level co-occurrence matrix in the texture evaluation of breast tumor on ultrasound images," *Medical physics*, vol. 34, no. 2, pp. 379–387, 2007.
- [12] D.-R. Chen, R.-F. Chang, C.-J. Chen, M.-F. Ho, S.-J. Kuo, S.-T. Chen, S.-J. Hung, and W. K. Moon, "Classification of breast ultrasound images using fractal feature," *Clinical imaging*, vol. 29, no. 4, pp. 235–245, 2005.
- [13] K. I. Laws, "Texture energy measures," in *Proc. Image understanding workshop*, 1979, pp. 47–51.
- [14] R. M. Haralick, K. Shanmugam, and I. H. Dinstein, "Textural features for image classification," *IEEE Transactions on systems, man, and cybernetics*, no. 6, pp. 610–621, 1973.
- [15] M. Nakagami, "The m-distribution—a general formula of intensity distribution of rapid fading," *Statistical Method of Radio Propagation*, 1960.
- [16] D. P. Hruska, "Improved techniques for statistical analysis of the envelope of backscattered ultrasound using the homodyned k distribution," *Master's thesis, University of Illinois at Urbana-Champaign*, 2009.
- [17] C. E. Shannon, "A mathematical theory of communication," *The Bell System Technical Journal*, vol. 27, pp. 379–423, 623–656, July, October 1948.